Available online at www.sciencedirect.com
SCIENCE DIRECT
International Journal of Heat and Mass Transfer 49 (2006) 1489–1492
International Journal of HEAT and MASS TRANSFER
www.elsevier.com/locate/ijhmt

A partial shrinkage model for selective laser sintering of a two-component metal powder layer

Tiebing Chen, Yuwen Zhang *

Department of Mechanical and Aerospace Engineering, University of Missouri-Columbia, Columbia, MO 65211, United States

Received 8 April 2005; received in revised form 6 September 2005
Available online 23 November 2005

Abstract

A partial shrinkage model for selective laser sintering of a metal powder mixture that contains two kinds of metal powders with significantly different melting points is developed. Laser-induced melting accompanied by partial shrinkage, liquid metal flow driven by capillary and gravitational forces, and resolidification of the metal powder layer are modeled using a temperature transforming model. The effect of volume fraction of the gas in the sintered region on the sintering process is investigated.

1. Introduction

Selective laser sintering (SLS) of metal powder is a layered manufacturing method that creates solid, three-dimensional objects by fusing powdered materials with a directed laser beam [1]. Melting and resolidification are the mechanisms to bond metal powder particles to form a layer of part and to bond different layers together to form a functional part. Fundamentals of melting and solidification have been investigated extensively and detailed reviews are available in the literatures [2,3]. Significant density change induced by shrinkage accompanies melting in the SLS of the two-component metal powders since the high melting point powder alone cannot sustain the structure of the powder layer. In addition, the liquid flow of the molten metal in the liquid pool due to capillary and gravitational forces also needs to be considered.

Pak and Plumb presented a one-dimensional thermal model of melting of the two-component powder bed, in which the liquid flow driven by capillary and gravitational forces is considered. Zhang et al. [5] developed a three-dimensional thermal model of SLS of two-component metal powder bed and convection driven by capillary and gravitational forces was taken into account. It was assumed that all the gas initially in the powder bed is driven out upon melting of low melting point metal powder and the heat affected zone (HAZ) was fully densified. The thickness of the powder bed used in Ref. [5] was very large, which approximated the sintering process of the first layer with the complete shrinkage. Melting and resolidification of a 3-D metal powder layer with a finite thickness heated by a moving Gaussian laser beam was investigated numerically by Chen and Zhang [6].

Since the lifespan of the liquid pool in the SLS is very short, the powder bed may not have sufficient time to achieve complete shrinkage. The rate of the shrinkage in the SLS process may be between the complete shrinkage and no shrinkage. A partial shrinkage model of SLS of two-component metal powder will be developed and the effects of partial shrinkage on the SLS process will be investigated.

2. Partial shrinkage model

The physical model of the problem under consideration is shown in Fig. 1. A Gaussian laser beam scans the surface of a two-component metal powder layer with a constant velocity, u_b. A coordinate system whose origin is fixed at

* Corresponding author. Tel.: +1 573 884 6936; fax: +1 573 884 5090.
E-mail address: Zhangyu@missouri.edu (Y. Zhang).

0017-9310/$ - see front matter © 2005 Elsevier Ltd. All rights reserved.
doi:10.1016/j.ijheatmasstransfer.2005.09.027

Nomenclature

Bi	Biot number, hR/k_H
C	dimensionless heat capacity, C^0/C^0_H
I_0	laser intensity at the center, (W/m^2)
K	dimensionless thermal conductivity, k/k_H
N_i	dimensionless laser intensity, $\alpha_a I_0 R/[k_H(T^0_m - T^0_i)]$
N_R	radiation number, $\varepsilon_e\sigma(T^0_m - T^0_i)^3 R/k_H$
N_t	temperature ratio for radiation, $T^0_m/(T^0_m - T^0_i)$
R	radius of the moving laser beam at 1/e (m)
s	solid–liquid interface location (m)
s_0	location of surface (m)
s_{st}	sintered depth (m)
T	dimensionless temperature, $(T^0 - T^0_m)/(T^0_m - T^0_i)$
T_0	dimensionless surface temperature
T^0	temperature (K)
U_b	dimensionless heat source moving velocity, $u_b R/\alpha_H$
$\mathbf{V}$	dimensionless velocity vector, $\mathbf{v}R/\alpha_H$
X, Y, Z	dimensionless moving horizontal coordinate, $(x, y, z)/R$

Greek symbols

α	thermal diffusivity (m^2 s^{-1})
α_a	absorptivity
Δ	dimensionless powder layer thickness, δ/R
ε	porosity
η	dimensionless location of the solid–liquid interface, s/R
η_0	dimensionless location of the surface, s_0/R
η_{st}	dimensionless sintered depth, s_{st}/R
τ	dimensionless false time, $\alpha_H t/R^2$
φ	volume fraction

Subscripts

g	gas(es)
H	high melting point powder
i	initial
ℓ	liquid or sintered region
L	low melting point powder
s	solid of low melting point powder

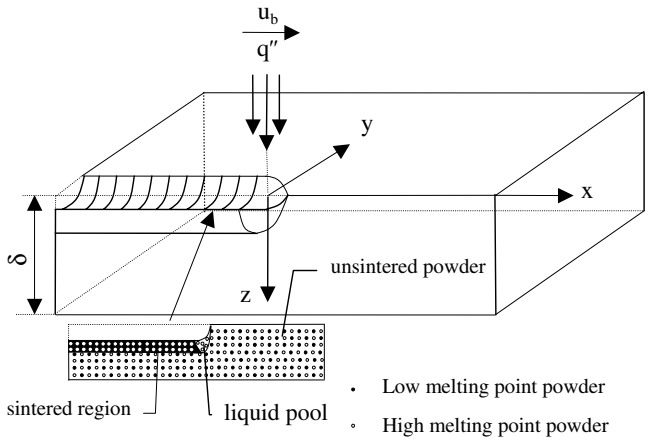

Fig. 1. Physical model.

the center of the laser beam is employed and the problem appears to be steady-state in the moving coordinate system. The initial temperature of the powder layer, T_i, is below the melting point of the low melting point powder, T_m. As the laser beam interacts with the powders, the temperature of the powders is brought up to T_m and then melting occurs. A liquid pool is formed under the laser beam and the melt infiltrates the unsintered powders driven by capillary and gravitational forces.

The loose powder bed contains high melting point powder (H), low melting point powder (s), and gas (g,s; gas in loose powder); the volume fraction of all components add up to unity, i.e., $\varphi_H + \varphi_s + \varphi_{g,s} = 1$. Upon melting, the liquid pool contains high melting point powder (H), liquid (ℓ) of low melting point component, and gas (g, ℓ; gas in liquid region) and their volume fractions satisfies $\varphi_H + \varphi_\ell + \varphi_{g,\ell} = 1$; this relationship is also applicable in the resolidified region if φ_ℓ also represents volume fraction of the resolidified low melting point component. The porosity, ε, defined as volume fraction of void that can be occupied by either gas or liquid, is equal to $\varphi_{g,s}$ in the loose powder and it becomes $\varphi_\ell + \varphi_{g,\ell}$ after melting. If the volume of the gas being driven out from the powder bed is equal to the volume of the liquid generated during melting, the porosity of the powder bed before and after melting will be the same, i.e., $\varepsilon = \varphi_{g,s} = \varphi_s + \varphi_{g,\ell}$, which is referred to as constant porosity model [4,5]. If the volume fractions of high and low melting point powders before sintering satisfy $\varphi_s/(\varphi_H + \varphi_s) = \varphi_{g,s}$, the powder bed can be fully densified ($\varphi_{g,\ell} = 0$) under constant porosity model [5,6]. On the other hand, if there is no shrinkage, one would expect that $\varphi_{g,\ell} = \varphi_{g,s}$ and the porosity, ε, will increase because φ_ℓ increases during melting. The complete shrinkage under constant porosity model and no shrinkage represent two extremes in SLS of two-component metal powders. Under the partial shrinkage model to be developed, the different shrinkage rates during melting is represented by the volume fraction of gas in the liquid pool, $\varphi_{g,\ell}$.

The problem is formulated using a temperature transforming model [7]. The dimensionless energy equation and corresponding initial and boundary equations are

$$\nabla\cdot(\varphi_\ell \mathbf{V}_\ell C_L T) - U_b\frac{\partial}{\partial X}[(\varphi_H+\varphi_s C_L)T] + W_s\frac{\partial}{\partial Z}[(\varphi_H+\varphi_s C_L)T] = \nabla\cdot(K\nabla T) - \left\{\frac{\partial}{\partial\tau}[(\varphi_\ell+\varphi_s)S] + \nabla\cdot(\varphi_\ell\mathbf{V}_\ell S) + W_s\frac{\partial}{\partial Z}(\varphi_s S) - U_b\frac{\partial}{\partial X}[(\varphi_\ell+\varphi_s)S]\right\} \quad (1)$$

$$-K\frac{\partial T}{\partial Z} = N_i\exp(-X^2-Y^2) - N_R[(T+N_t)^4-(T_\infty+N_t)^4] - Bi(T-T_\infty) \quad Z=\eta_0(X) \quad (2)$$

$$\frac{\partial T}{\partial Z}=0, \quad Z=\Delta \quad (3)$$

$$\frac{\partial T}{\partial X}=0, \quad |X|\to\infty \quad (4)$$

$$\frac{\partial T}{\partial Y}=0, \quad |Y|\to\infty \quad (5)$$

where the dimensionless heat capacity, C, source term, S, and thermal conductivity, K, and the dimensionless velocities of the liquid phase, $\mathbf{V}_\ell$, are available in Ref. [5,6] and will not be repeated here.

The dimensionless continuity equation of the liquid is

$$\frac{\partial\varphi_\ell}{\partial\tau} - U_b\frac{\partial\varphi_\ell}{\partial X} + \nabla\cdot(\varphi_\ell\mathbf{V}_\ell) = \dot{\Phi}_L \quad (6)$$

where $\dot{\Phi}_L$ is dimensionless volume production rate of liquid.

Assuming shrinkage occurs in the z-direction only, the continuity equations for the solid phase of the low melting point powder and high melting point powder are

$$\frac{\partial\varphi_s}{\partial\tau} - U_b\frac{\partial\varphi_s}{\partial X} + \frac{\partial(\varphi_s w_s)}{\partial Z} = -\dot{\Phi}_L \quad (7)$$

$$\frac{\partial\varphi_H}{\partial\tau} - U_b\frac{\partial\varphi_H}{\partial X} + \frac{\partial(\varphi_H w_s)}{\partial Z} = 0 \quad (8)$$

and the following relationship is valid in all regions

$$\varepsilon+\varphi_s+\varphi_H = 1 \quad (9)$$

Adding Eqs. (7) and (8) together and considering Eq. (9), an equation about volume production rate is obtained:

$$\dot{\Phi}_L = -\frac{\partial(1-\varepsilon)}{\partial\tau} + U_b\frac{\partial(1-\varepsilon)}{\partial X} - \frac{\partial}{\partial Z}[(1-\varepsilon)W_s] \quad (10)$$

Under the constant porosity model discussed in Ref. [6], only the third term on the right-hand side of Eq. (10) was present. Under the partial shrinkage model, the porosity, ε, is not constant and the first two terms on the right-hand side of Eq. (10) are necessary. Since the shrinkage only occurs at the interface between liquid pool and the unsintered region, the velocity induced by shrinkage, W_s, is a constant in z-direction within the liquid pool and is equal to zero in the unsintered region. The velocity induced by shrinkage in the liquid pool can be obtained by integrating Eq. (8) and the result is

$$W_s = \begin{cases} 0, & Z>S \\ \frac{1-\varepsilon_\ell-\varphi_{H,i}}{1-\varepsilon_\ell}\left(\frac{\partial S}{\partial\tau} - U_b\frac{\partial S}{\partial X}\right), & Z<S \end{cases} \quad (11)$$

where $\varphi_{H,i}$ is initial volume fraction of the high melting point powder, and $\varepsilon_\ell=\varphi_\ell+\varphi_{g,\ell}$ is the porosity in the liquid pool (including resolidified region).

The governing equations are discretized by a finite volume method [8] and solved numerically. The powder bed, which includes unsintered powder, a liquid pool, and sintered region, has an irregular shape since the upper surface of the powder bed recedes due to shrinkage. A block-off approach [8] is employed to deal with the irregular geometric shape and the thermal conductivity in the empty space created by the shrinkage is zero. The computation was carried out using a non-uniform grid in the X and Y-directions and uniform grid in the Z-direction. The grid number used in the numerical simulation was $168\times37\times22$.

3. Results and discussion

The effects of the different volume fraction of the gas in the liquid and resolidified regions, $\varphi_{g,\ell}$, on the shape of

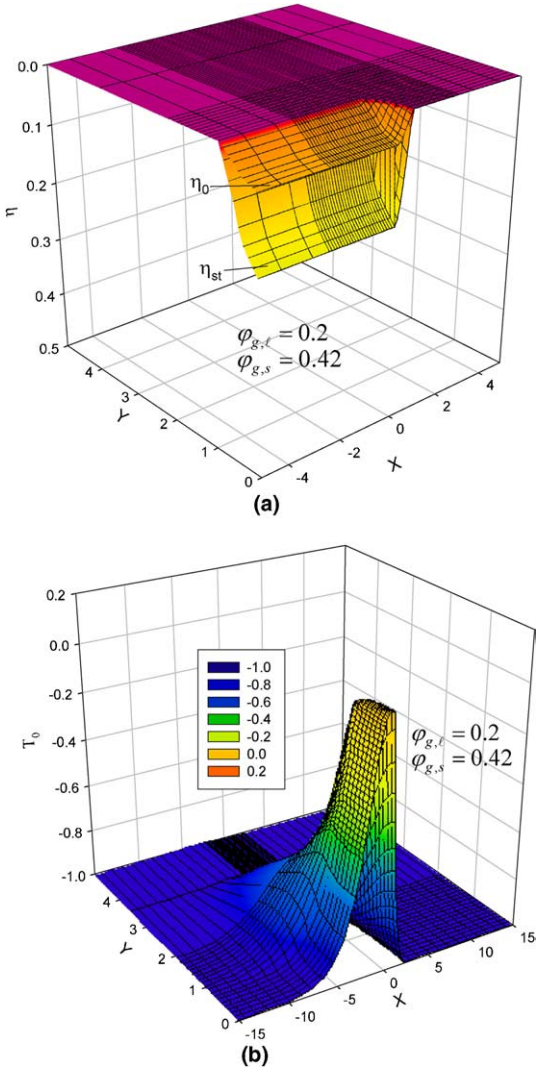

Fig. 2. Three-dimensional shape of the HAZ and surface temperature distribution ($\Delta=0.25$, $\varphi_{g,\ell}=0.2$, $\varphi_{g,s}=0.42$).

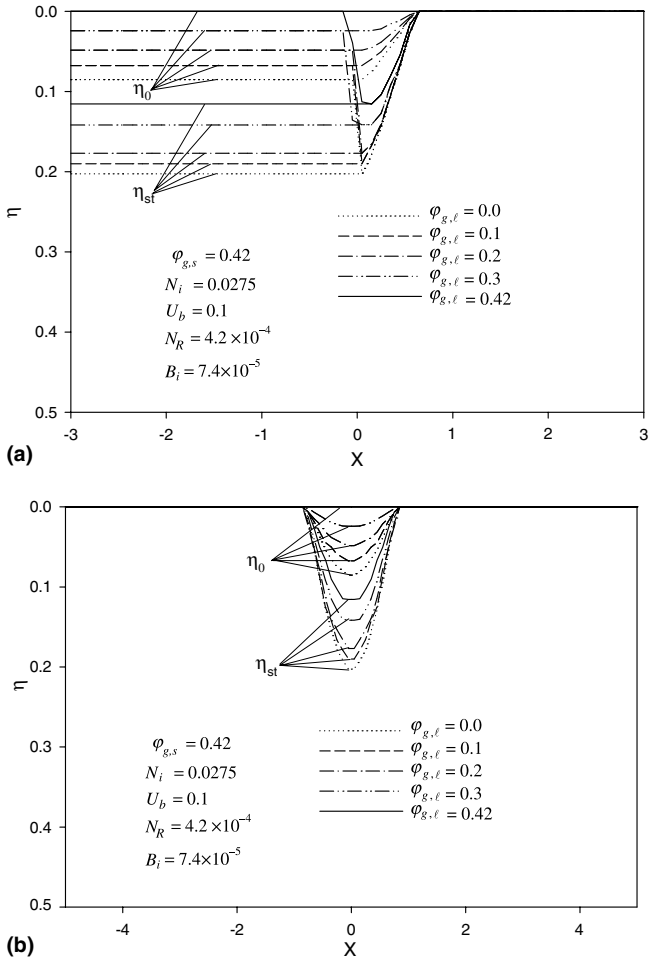

Fig. 3. Effect of $\varphi_{g,\ell}$ on the HAZ.

HAZ are investigated. The initial porosity of the powder, $\varphi_{g,s}$, was chosen to be 0.42 based on a simple mass/volume measurement procedure by Zhang et al. [5]. The three-dimensional shape of HAZ and corresponding surface temperature distribution for $\varphi_{g,\ell} = 0.2$ are shown in Fig. 2(a) and (b), respectively. There is still gas remaining in HAZ when the partial shrinkage occurs. The void space above the top surface is generated due to the shrinkage of the powder layer during melting. Fig. 2(b) shows the surface temperature distribution of the powder layer. The temperature at the top surface of the liquid pool is above the melting point of the low melting point powder and decreases rapidly when the distance from the center of the laser beam increases.

The effects of $\varphi_{g,\ell}$ on the shape and size of HAZ are demonstrated using the longitudinal and cross-sections of HAZ shown in Fig. 3. The cases of the complete shrinkage ($\varphi_{g,\ell} = 0$), no-shrinkage ($\varphi_{g,\ell} = 0.42$) and partial shrinkages in between were investigated. For giving dimensionless laser beam intensity and scanning velocity, the sintering depth increases with decreasing $\varphi_{g,\ell}$. The size of the liquid pool is also growing with decreasing $\varphi_{g,\ell}$, because lower $\varphi_{g,\ell}$ results in higher thermal conductivity in the liquid. The largest sintering depth and size of HAZ are obtained when $\varphi_{g,\ell}$ is equal to zero, i.e., the complete shrinkage. In order to obtain the same sintering depth, the larger laser power or lower scanning velocity are needed for larger $\varphi_{g,\ell}$. The comparison between the numerical solution for the complete shrinkage and experimental result was performed by the authors [6]; the cross-section of the HAZ in the simulation result approximately 20% was larger than that of the experimental result because the HAZ was porous in the experimental results. The cross-sectional area of the HAZ predicted by using the partial shrinkage model with $\varphi_{g,\ell} = 0.2$ agreed very well with the experimental results.

4. Conclusion

A partial shrinkage model for selective laser sintering of the two-component metal powders is developed and the effects of the volume fraction of the gas in the liquid or sintered regions, $\varphi_{g,\ell}$, on the shape and size of heat affected zone (HAZ) were investigated. The results indicate that the sintering depth and volume of HAZ significantly increases with decreasing $\varphi_{g,\ell}$.

Acknowledgement

Support for this work by the Office of Naval Research (ONR) under grant number N00014-04-1-0303 is gratefully acknowledged.

References

[1] J. Conley, H. Marcus, Rapid prototyping and solid freeform fabrication, J. Manufact. Sci. Eng. 119 (1997) 811–816.
[2] R. Viskanta, Phase change heat transfer, in: G.A. Lane (Ed.), Solar Heat Storage: Latent Heat Materials, CRC Press, Boca Raton, FL, 1983.
[3] L.C. Yao, J. Prusa, Melting and freezing, Adv. Heat Transfer 25 (1989) 1–96.
[4] J. Pak, O.A. Plumb, Melting in a two-component packed bed, J. Heat Transfer 119 (1997) 553–559.
[5] Y. Zhang, A. Faghri, C.W. Buckley, T.L. Bergman, Three-dimensional sintering of two-component metal powders with stationary and moving laser beams, J. Heat Transfer 122 (2000) 150–158.
[6] T. Chen, Y. Zhang, Three-dimensional modeling of selective laser sintering of two-component metal powder layers, J. Manufact. Sci. Eng. 128 (2006), in press.
[7] Y. Cao, A. Faghri, A numerical analysis of phase change problems including natural convection, J. Heat Transfer 112 (1990) 812–816.
[8] S.V. Patankar, Numerical Heat Transfer and Fluid Flow, McGraw-Hill, New York, 1980.